ORIGINAL RESEARCH

Transplantation of Mesenchymal Stem Cells Attenuates Pulmonary Hypertension by Normalizing the Endothelial-to-Mesenchymal Transition

Junyi Huang[1]*, Wenju Lu[1]*, Haiping Ouyang[1]*, Yuqin Chen[1]*, Chenting Zhang[1], Xiaoyun Luo[1], Meichan Li[1], Jiaze Shu[1], Qiuyu Zheng[1], Haixia Chen[1], Jiyuan Chen[1], Haiyang Tang[1,2], Dejun Sun[3], Jason X.-J. Yuan[1,2], Kai Yang[1‡], and Jian Wang[1,2,3‡]

[1]State Key Laboratory of Respiratory Disease, National Clinical Research Center for Respiratory Disease, Guangdong Key Laboratory of Vascular Disease, Guangzhou Institute of Respiratory Health, the First Affiliated Hospital of Guangzhou Medical University, Guangzhou, Guangdong, China; [2]Division of Translational and Regenerative Medicine, the University of Arizona College of Medicine, Tucson, Arizona; and [3]Division of Pulmonary and Critical Care Medicine, the People's Hospital of Inner Mongolia, Huhhot, Inner Mongolia, China

Abstract

For decades, stem cell therapies for pulmonary hypertension (PH) have progressed from laboratory hypothesis to clinical practice. Promising preclinical investigations have laid both a theoretical and practical foundation for clinical application of mesenchymal stem cells (MSCs) for PH therapy. However, the underlying mechanisms are still poorly understood. We sought to study the effects and mechanisms of MSCs on the treatment of PH. For *in vivo* experiments, the transplanted GFP^+ MSCs were traced at different time points in the lung tissue of a chronic hypoxia–induced PH (CHPH) rat model. The effects of MSCs on PH pathogenesis were evaluated in both CHPH and sugen hypoxia–induced PH models. For *in vitro* experiments, primary pulmonary microvascular endothelial cells were cultured and treated with the MSC conditioned medium. The specific markers of endothelial-to-mesenchymal transition (EndMT) and cell migration properties were measured. MSCs decreased pulmonary arterial pressure and ameliorated the collagen deposition, and reduced the thickening and muscularization in both CHPH and sugen hypoxia–induced PH rat models. Then, MSCs significantly attenuated the hypoxia-induced EndMT in both the lungs of PH models and primary cultured rat pulmonary microvascular endothelial cells, as reflected by increased mesenchymal cell markers (fibronectin 1 and vimentin) and decreased endothelial cell markers (vascular endothelial cadherin and platelet endothelial cell adhesion molecule-1). Moreover, MSCs also markedly inhibited the protein expression and degradation of hypoxia-inducible factor-2α, which is known to trigger EndMT progression. Our data suggest that MSCs successfully prevent PH by ameliorating pulmonary vascular remodeling, inflammation, and EndMT. Transplantation of MSCs could potentially be a powerful therapeutic approach against PH.

Keywords: mesenchymal stem cells; pulmonary hypertension; endothelial-to-mesenchymal transition

(Received in original form May 3, 2018; accepted in final form June 14, 2019)

*These authors contributed equally to this work and share first authorship.

‡These authors contributed equally to this work and share senior authorship.

Supported in part by National Natural Science Foundation of China grants 81630004, 81470246, 81220108001, 81520108001, 81770043, 81800054, 81800057, and 81800061, Department of Science and Technology of China grants 2016YFC0903700 and 2016YFC1304102, Changjiang Scholars and Innovative Research Team in University grant IRT0961, Local Innovative and Research Teams Project of Guangdong Pearl River Talents Program grant 2017BT01S155, Guangdong Department of Science and Technology grants 2016A030311020, 2016A030313606, and 2017A020215114, Guangzhou Department of Education Yangcheng scholarship 12A001S, Guangzhou Department of Education scholarship 1201630095, Guangzhou Department of Science and Technology grants 2014Y2-00167 and 201607010358, the Guangdong Province Universities and Colleges Pearl River Scholar Funded Scheme of China, the Inner Mongolia Autonomous Region science and technology innovation guidance project, and the Inner Mongolia Autonomous Region science and technology project 20160298. This work was also supported in part by National Heart, Lung, and Blood Institute of the National Institutes of Health grants R35HL135807 and U01HL125208 and an Actelion ENTELLIGENCE Young Investigator Award.

Author Contributions: J.W. initiated and designed the project, analyzed data and edited the manuscript. K.Y. contributed to the design, revision of the project, and editing of the manuscript. W.L. and J.X.-J.Y. contributed to the design of the project. J.H. performed the animal and cell experiments, analyzed data, and wrote the manuscript. H.O. and Y.C. contributed to the molecular and animal experiments. C.Z. performed the animal and functional experiments. X.L., M.L., J.S., Q.Z., H.C., and J.C. contributed to the molecular experiments. H.T. and D.S. provided consultation and advice on the project and edited the manuscript. All authors agreed to the final submission of the manuscript.

Correspondence and requests for reprints should be addressed to Jian Wang, Ph.D., State Key Laboratory of Respiratory Disease, Guangzhou Institute of Respiratory Health, The First Affiliated Hospital of Guangzhou Medical University, 151 Yanjiang Road, Guangzhou, Guangdong 510120, People's Republic of China. E-mail: jianwang1@email.arizona.edu.

This article has a data supplement, which is accessible from this issue's table of contents at www.atsjournals.org.

Am J Respir Cell Mol Biol Vol 62, Iss 1, pp 49–60, Jan 2020

Originally Published in Press as DOI: 10.1165/rcmb.2018-0165OC on June 18, 2019
Internet address: www.atsjournals.org

Pulmonary hypertension (PH) is a progressive, fatal disease syndrome, which results in increased pulmonary vascular resistance and pulmonary pressure, right ventricular (RV) hypertrophy, heart failure, and even death (1). As is well known, PH is characterized by a series of structural changes in the pulmonary arteries (PAs), including increased adventitial and medial thickness, eccentric and concentric intimal thickening, and *in situ* thrombosis. In the vascular lesions, increased numbers of ACTA2-positive cells were thought to be responsible for the vascular remodeling (2). It has been traditionally thought that such smooth muscle (SM)–like cells were derived from proliferative expansion of the dedifferentiation of resident vascular media SM cells or the differentiation of adventitial fibroblasts (3). However, in addition to the adventitial and medial, many investigators have recently turned to the resident endothelial cells within the intima, which may delaminate from their organized layer of cells in the vessel lining, transition to mesenchymal or SM-like phenotype in a process called endothelial-to-mesenchymal transition (EndMT), and migrate to their underlying tissue (4).

EndMT is a process of endothelial cells transformed into mesenchymal cells, by which endothelial cells lose their endothelial characteristics and gain a mesenchymal-like phenotype (4). Recent studies have proved that loss of endothelial cell–cell contacts is a trigger for EndMT. Many factors or stimuli, such as hypoxia and inflammation, initiate the loss of cell–cell contacts through activating metalloproteinase and serine protease family members. HIF-2α (hypoxia-inducible factor-2α) has recently been proven to upregulate the expression of members of the SNAI family, such as Snail 1/2 (5), which is one of the transcription factors actively involved in suppression of endothelial-specific proteins (VE [vascular endothelial]-cadherin, PECAM [platelet endothelial cell adhesion molecule]-1, etc.) and upregulation of mesenchymal-specific proteins (fibronectin [FN] 1, vimentin, etc.), after the interruption of cell–cell or cell–matrix contact. The recent discoveries of EndMT in different diseases suggest that modulation of EndMT may represent a promising new treatment strategy (2–4, 6).

Possible mechanisms for the therapeutic role of mesenchymal stem cells (MSCs) include: *1*) cell replacement—transplanted MSCs differentiate into damaged tissue cells for tissue damage repair; *2*) paracrine mechanisms—transplanted MSCs promote the healing of wounds by secreting biologically active substances; *3*) immunoregulation mechanisms—MSCs have capabilities of self-renewal and multidirectional differentiation for therapeutic purposes. Due to their low immunogenicity, multilineage potential, and scalability for clinical trials, MSCs seem to be an ideal cell type for developing stem cell–based therapeutic strategies (7). Indeed, studies in an MCT-PH rat model have indicated that transplantation of MSCs would attenuate PA pressures, RV hypertrophy, and pulmonary vascular remodeling (8–11). Interestingly, some researchers believe that only a small population of the MSCs can differentiate into target cells and the process is relatively slow (10). In recent years, experimental studies and clinical trials have shown that MSC-mediated therapeutic benefits may depend, to a large extent, on the secretion of growth factors and cytokines (12). Therefore, the paracrine mechanism of MSCs is believed to play an essential therapeutic role despite low levels of cell persistence. Some researchers have reported that MSC treatment can attenuate EndMT in a variety of diseases, such as myocardial infarction and unilateral ureteral obstruction (13, 14). Thus, based on these previous observations, whether MSCs could also affect the EndMT during PH and if MSC-based transplantation has the potential to lead to a new avenue in PH therapy remain open questions.

In this study, we assessed the effects of MSCs on the development of PH in both chronic hypoxia (CH)–induced PH (CHPH) and sugen hypoxia–induced (SuHx) PH (SuHx-PH) rat models, as well as in primarily isolated and cultured rat pulmonary microvascular endothelial cells (PMECs), to comprehensively evaluate the potential therapeutic roles of MSC transplantation on these two well-established PH models, and validate the potential regulation of MSCs on the EndMT during PH pathogenesis.

Methods

Culture of MSCs

Bone marrow–derived MSCs of Sprague-Dawley rat (Cyagen Bioscience) were purchased at passage 2. The details of characterization and culture methods are provided in the data supplement. Cells at passage 3–6 were used for experimentation.

Animal Model

The CHPH rat model has been well established and used by our group extensively in previously published work (15, 16). Descriptions of the SuHx-PH rat model and the hypoxic exposure and treatment protocols are provided in the data supplement (see also Figure E2 in the data supplement). All procedures were approved by the Animal Care and Use Committee of Guangzhou Medical University.

Hemodynamic Parameter Measurement and Histological Staining

RV systolic pressure (RVSP) was measured using the same methods as we described previously (17). Intrapulmonary vessels were visualized by histological staining on formalin-fixed and paraffin-embedded lung cross-sections of 5 μm thickness. Details are provided in the data supplement.

Lung Tissue Immunofluorescence and Flow Cytometry Analysis

Lung tissue immunofluorescence was performed as previously described. Details are provided in the data supplement.

Hydroxyproline Assay

The protein levels of hydroxyproline in lung tissue homogenates were measured by hydroxyproline assay kits (Abcam). Details are provided in the data supplement.

MSC Conditioned Medium Preparation

MSCs at passage 3–6 were grown to greater than 80% confluency, the medium discarded, and the cells rinsed three times with PBS. Cells were then cultured with serum-free medium (Eagle's minimum essential medium [α-MEM]) for 24 hours. After 24 hours, supernatants from MSC cultures were collected and centrifuged at 5,000 rpm for 5 minimum to remove remaining cells. MSC conditioned medium (MSC-CM) was collected and filtered through a 0.22-μm filter to remove cellular debris. MSC-CM was temporarily frozen at −20°C. Serum-free α-MEM was the vehicle control.

The Culture and Treatment of Rat PMECs

Rat PMECs were cultured and identified as previously described (5). The hypoxic exposure and treatment protocols are provided in the data supplement.

RNA Extraction, cDNA Generation, and Quantitative PCR

Total RNA was isolated from frozen tissue and cells using TRIZOL reagent (Invitrogen) as previously described (18, 19). Quantitative PCR was performed using Scofast EvaGreen SuperMix (Bio-Rad) in a CFX96 real-time system (Bio-Rad) according to the manufacturer's instruction. Details are provided in the data supplement.

Western Blot

Both rat lung tissues and PMECs were sonicated and lysed in radioimmunoprecipitation assay buffer (RIPA buffer) (GBCBIO Technologies) containing 1% PMSF and protease inhibitor cocktail II and III. Total protein concentrations were measured by a BCA protein assay kit (Pierce). After being denatured with the addition of a loading buffer and heating at 100°C for 10 minutes, protein expression was measured by IB assay as previously described (15, 17, 20). Details are provided in the data supplement.

Cell Migration Assay

To quantify cell migration, Transwell polycarbonate filter with 8-μm pores was used in our study. Details are provided in the data supplement.

Statistical Analysis

The results are expressed as means (±SEM) from at least five independent experiments. The statistical differences between two or more different experimental groups were determined using Student's *t* test or one-way ANOVA, as appropriate. Differences were considered to be significant at a *P* value less than 0.05.

Results

Homing of Intravenously Injected MSCs in CHPH Rats

To determine the homing distribution of MSCs, cells were labeled with GFP by lentiviral transfection, and lung sections of CHPH and normal rats were obtained 3 hours, 1 day, 3 days, 7 days, and 14 days after intravenous injection, as was the flow cytometry of GFP^+ cells. As shown in Figures 1A and 1B, the number of positive cells in the lung reached a peak at Day 7 (18.2 cells/high-magnification field) after the MSC administration, and gradually decreased at Day 14 (9.8 cells/high-magnification field). Compared with the normoxic control group, the number of GFP^+ cells was much higher in the lungs of CHPH rats, indicating that MSCs are more likely homing to the injured tissues. In parallel, we observed a similar pattern by using flow cytometry (Figure 1C). However, by double staining of GFP (green) and von Willebrand factor (vWF; red), we did not find obvious colocalization of MSCs with the pulmonary vasculature, suggesting that the transplanted MSCs were distributed throughout the lung tissue rather than accumulating around the vessels and differentiating into endothelial cells (Figure 1D).

MSCs Decreased RV Pressure and Remodeling in CHPH and SuHx-PH Rat Models

As shown in Figure 2, rats exposed to CH (10% O_2, 21 d) established typical PH pathogenesis, characterized by elevated RVSP, RV hypertrophy (RV/(LV + S)), and distal PA remodeling (Figures 2A and B). Similar results were also obtained in the SuHx model rats (Figures 2C and D). However, in the CHPH rat model, transplantation of MSCs (CH + MSC) decreased the RVSP to 36.10 (±2.02) mm Hg (compared with 44.58 ± 1.97 mm Hg in the CH group; $P < 0.01$; $n = 7$–15) and normalized the RV/(LV + S) to 0.402 (±0.01) (compared with 0.462 ± 0.02 in the CH group; $P < 0.01$; $n = 7$–15). In parallel, we measured the effects of MSCs by using the SuHx-PH model, which showed even more significant therapeutic effects on the PH index. In detail, the RVSP decreased to 42.96 (±1.56) mm Hg in SuHx plus MSCs (compared with the SuHx group: 61.56 ± 4.33 mm Hg; $P < 0.01$; $n = 10$–14), RV/(LV + S) to 0.441 (±0.02) (compared with the SuHx group: 0.527 ± 0.02; $P < 0.01$; $n = 10$–14). Histological staining showed a significant increase of the pulmonary vascular wall area and thickness after 21 days of CH exposure, whereas MSC treatment could significantly attenuate the CH-induced PA wall thickening and muscularization in all vessels with a diameter within the ranges of 0–25 μm, 25–50 μm, and 50–100 μm (Figures 2E, 2F, and 2I). MSC treatment also gained significant effects in the PA remodeling of SuHx-PH model rats, indicating that the MSC exerts its beneficial effects in both CHPH and SuHx-PH rat models (Figures 2G, 2H, and 2J). In comparison, there were no significant differences in the PH index and vascular wall thickness after transplantation of fibroblast in either the CHPH or SuHx-PH models.

MSCs Ameliorated the Collagen Deposition around the PA Vasculature in Both CHPH and SuHx-PH Rat Models

We then used Masson's trichrome to determine whether MSCs could impact the collagen deposition in both CHPH and SuHx-PH rat models. Collagen deposition was found in both the CHPH and SuHx-PH model rats. However, MSC treatment effectively attenuated the collagen deposition in both models, as indicated by reduced collagen-positive staining area (blue). Immunohistochemistry showed upregulation of MMP2 and MMP9 in both PH model groups, which was significantly reduced by MSC treatment (Figures 3A and 3F). We also examined the expression level of MMP2 and MMP9 at both mRNA (Figures 3B and 3G) and protein levels (Figures 3D, 3E, 3I, and 3J) in the lung tissues, which provided similar results as those obtained from immunohistochemistry. Then, as shown in Figures 3C and 3H, treatment of MSCs also markedly inhibited the increased levels of hydroxyproline of lung tissue from both the CHPH and SuHx-PH model rats. Collectively, these data indicate that MSCs can ameliorate the collagen deposition in both the CHPH and SuHx-PH rat models.

MSCs Reduced EndMT in the Lung Vasculature from Both CHPH and SuHx-PH Rats

To determine the presence of transitional EndMT cells in the endothelium of remodeled small PAs from both CHPH and SuHx-PH rats, the distribution and expression of mesenchymal cell marker, α-SMA (green fluorescent signals), and endothelial cell marker, vWF (red fluorescent signals), were analyzed by

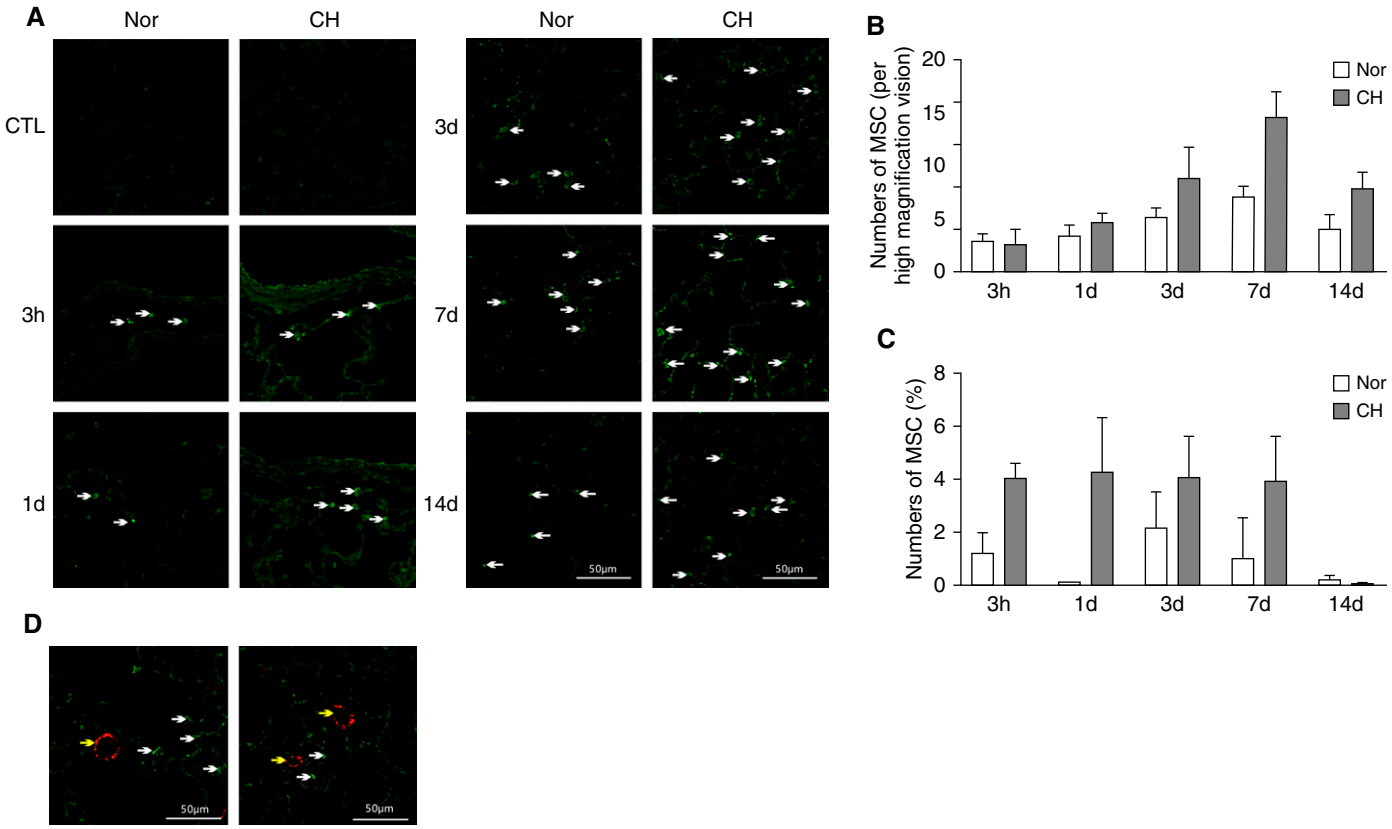

Figure 1. Distribution of intravenously injected mesenchymal stem cells (MSCs) in chronic hypoxia–induced pulmonary hypertension (CHPH) rats. MSCs were labeled with GFP and intravenously injected into CHPH and normoxia rats ($n = 5$). (*A*) Lung sections of CHPH and normoxic rats were obtained at 3 hours, 1 day, 3 days, 7 days, and 14 days after intravenous injection of GFP^+ MSC for observation of GFP^+ cells. (*B*) Bar graphs representing the number of positive cells (white arrows). (*C*) Bar graphs showing the GFP^+ cells determined by flow cytometry. (*D*) Immunofluorescence staining showing GFP^+ MSC (green staining, white arrows) with endothelial cell marker, von Willebrand factor (vWF; red staining, yellow arrows). Error bars represent means ± SEM. Scale bars: 50 μm. CTL = control; Nor = normoxia.

indirect immunofluorescence double-staining assay. As seen in Figure 4, double-positive staining for vWF and α-SMA (represented by merged yellow fluorescence) was distributed in the partial endothelium of remodeled small PAs in CHPH (Figure 4A) and SuHx-PH (Figure 4B) rats, and the colocalization was reduced upon the treatment of MSCs. Moreover, we observed significant upregulation of FN1, vimentin, Snail, and Twist1 as downregulation of VE-cadherin and PECAM-1 (CD31) at the protein level in the lung tissues of both CHPH (Figures 5A and 5B) and SuHx-PH (Figures 5C and 5D) rats, which can be reversed by MSC transplantation.

MSC-CM Attenuated Hypoxia-induced EndMT in Primary Cultured PMECs

To further validate the effects of MSCs on EndMT, primary cultured PMECs were treated with either MSC-CM or plain α-MEM control, then subjected to CH (3% O_2) for 7 days (Figure E2B). We found that hypoxia treatment induced the PMECs to transit into a fibroblast-like, spindle-shaped form compared with the cobble stone appearance of nontreated cells, and these changes were inhibited when incubated with MSC-CM (Figure 6A). Next, we detected the expression levels of both endothelial and mesenchymal markers in PMECs. As shown in Figures 6B and 6C, Western blot analysis revealed significant decreases in VE-cadherin and PECAM-1 protein expression in PMECs exposed to hypoxia compared with normoxic cells ($P < 0.05$), whereas incubation with MSC-CM significantly normalized these trends. In addition, hypoxia exposure significantly increased FN1, vimentin, and Snail protein expression in PMECs compared with normoxic cells ($P < 0.05$). This effect was significantly attenuated by treatment with MSC-CM. Vehicle control, which was treated with MSC basic medium, had no effect on the EndMT induced by hypoxia (Figures 6B and 6C).

MSC-CM Attenuated Hypoxia-induced Migration in Cultured PMECs

Because EndMT will induce cell migration and proliferation (21), transwell migration assays were performed in PMECs under normoxia and treated with or without MSC-CM under hypoxia. After 24 hours of hypoxia exposure, the ratio of migrated cells to total cells was increased in the hypoxia control group compared with the normoxic controls, whereas these changes were attenuated in the cotreatment with MSC-CM (Figure 6D), which suggests that hypoxia-induced migration in PMECs was decreased by MSC-CM.

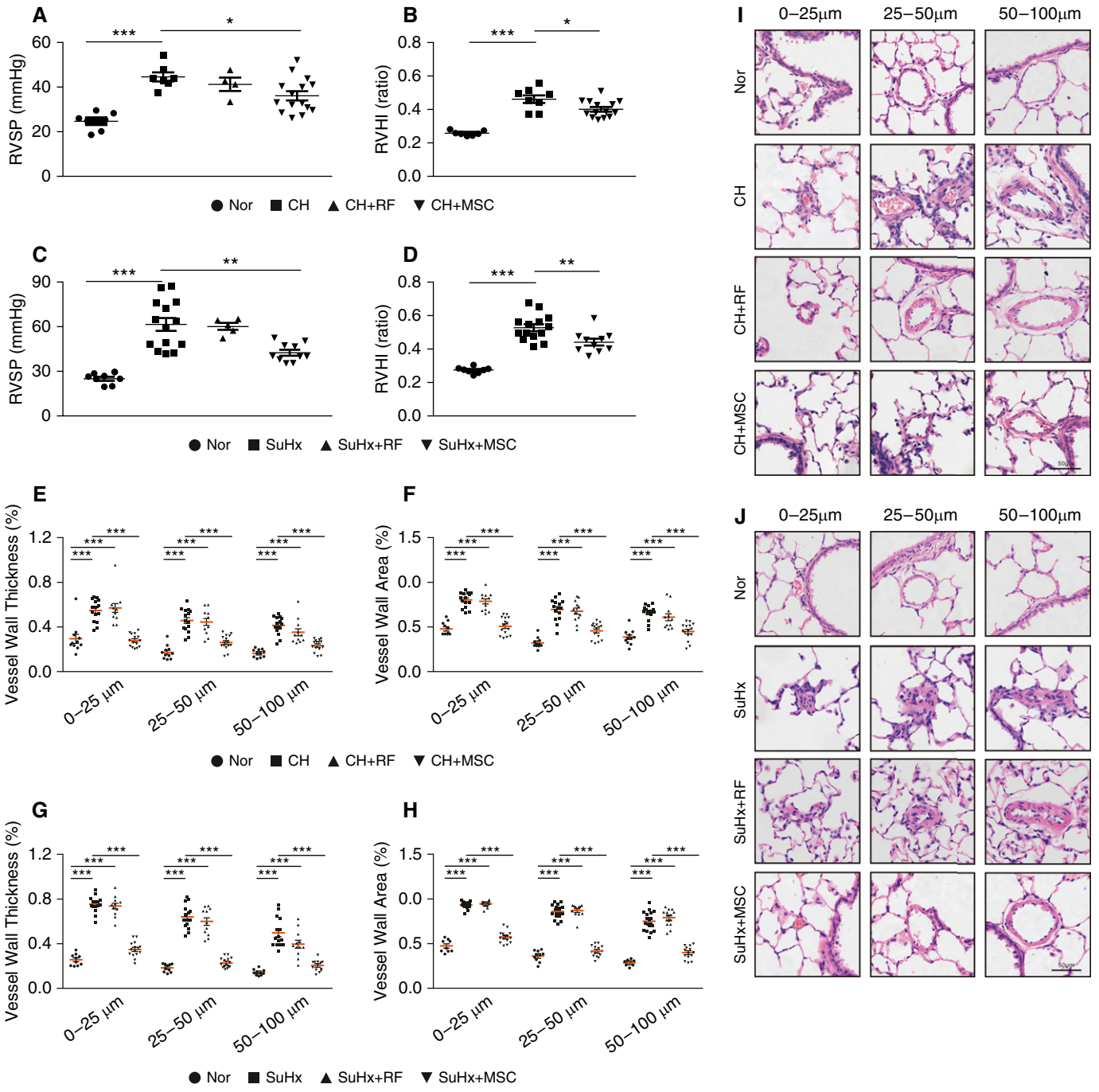

Figure 2. MSCs partially attenuated established PH in CHPH and sugen hypoxia–induced (SuHx) PH rat models. (*A–D*) Representing right ventricular (RV) systolic pressure (RVSP; *A* and *C*) and RV/(LV+S) (*B* and *D*) reflecting RV hypertrophy in the CHPH model (*A* and *B*) and the SuHx-PH model (*C* and *D*) rats treated with or without MSC. (*E–H*) Vessel wall thickness and vessel wall area of the distal pulmonary artery sections (in different diameter) from the CHPH model (*E* and *F*) and the SuHx-PH model (*G* and *H*). Error bars represent means ± SEM ($n = 7–15$ in each group). $^{*}P < 0.05$, $^{**}P < 0.01$, and $^{***}P < 0.001$. (*I* and *J*) Hematoxylin and eosin staining of the lung sections from both CHPH model (*I*) and SuHx-PH model rats (*J*). Scale bars: 50 μm. LV = left ventricle; RF = rat fibroblast; RVHI = right ventricular hypertrophy index; S = septum.

MSC-CM Inhibited Hypoxia-induced HIF-2α Expression by Promoting Its Protein Degradation

Because previous studies have proven that HIF-2α could contribute to the EndMT by upregulating the expression of Snail 1/2, we assumed that the suppression of MSCs on the expression of Snail is likely mediated by targeting HIF-2α expression or activity. As shown in Figure 7A, we found that, in both the CHPH and SuHx-PH model, the upregulation of HIF-2α protein in the lung tissue can be normalized by MSC transplantation. Moreover, as

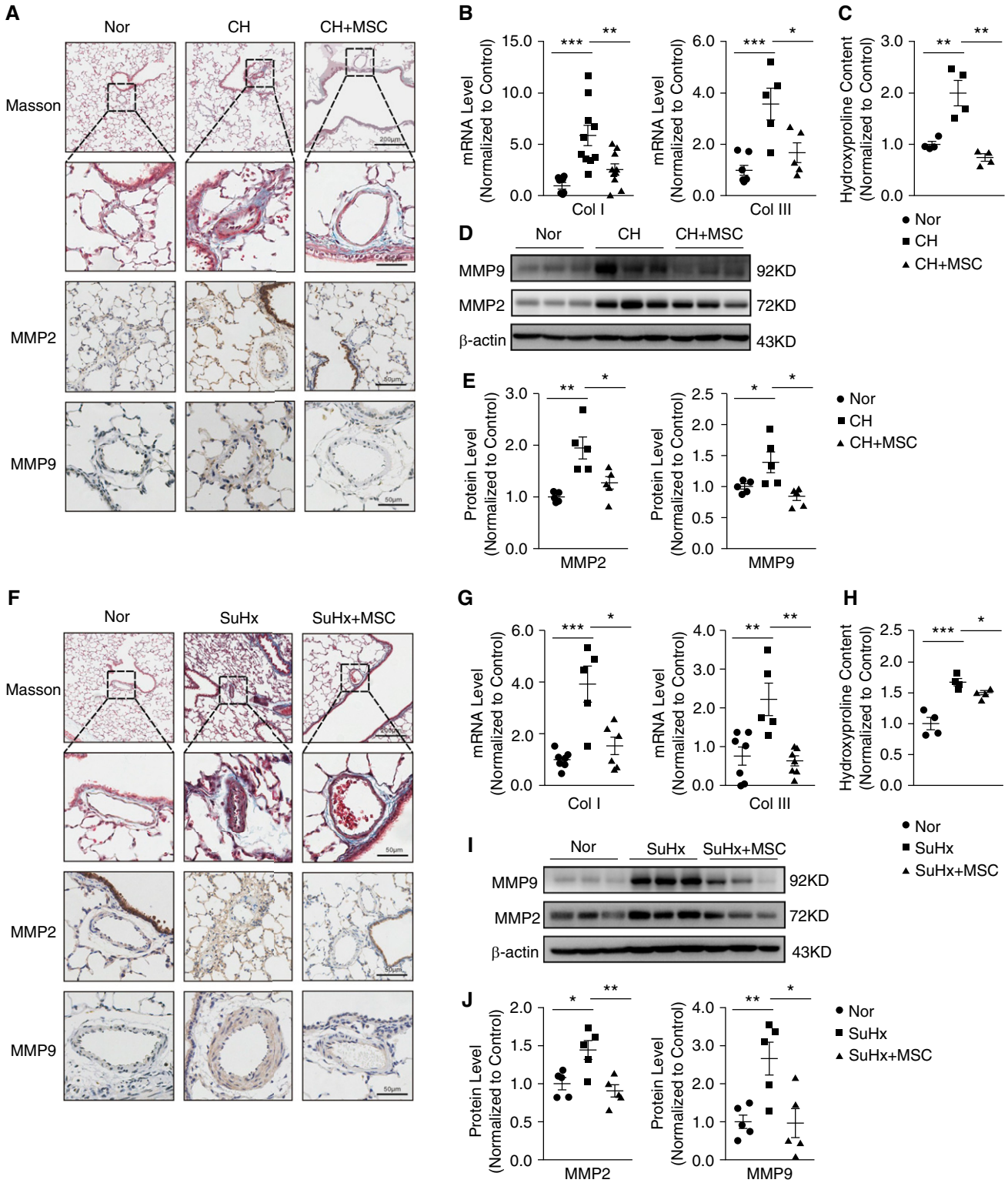

Figure 3. MSCs ameliorated the collagen deposition in the CHPH and SuHx-PH rat models. (*A* and *F*) Light-field microscopic analysis of Masson's trichrome staining and immunohistochemical staining for MMP2 and MMP9 expression of lung sections from normal rats and the CHPH/SuHx-PH models with or without MSC treatment. (*B* and *G*) mRNA expression of lung collagen I and collagen III from normal rats and CHPH/SuHx-PH models with or without MSC treatment (normalized to 18 s). (*C* and *H*) Protein level of hydroxyproline from normal rats and CHPH and SuHx-PH models with or without MSC treatment. (*D*, *E*, *I*, and *J*) Protein expression of lung MMP2 and MMP9 from normal rats and CHPH/SuHx-PH models with or without MSC treatment (*D*, *E*, *I*, and *J*). Error bars represent means ± SEM ($n = 5$ in each group). $^{*}P < 0.05$, $^{**}P < 0.01$, and $^{***}P < 0.001$. Scale bars: 50 μm and 200 μm. Col = collagen; MMP = matrix metallopeptidase.

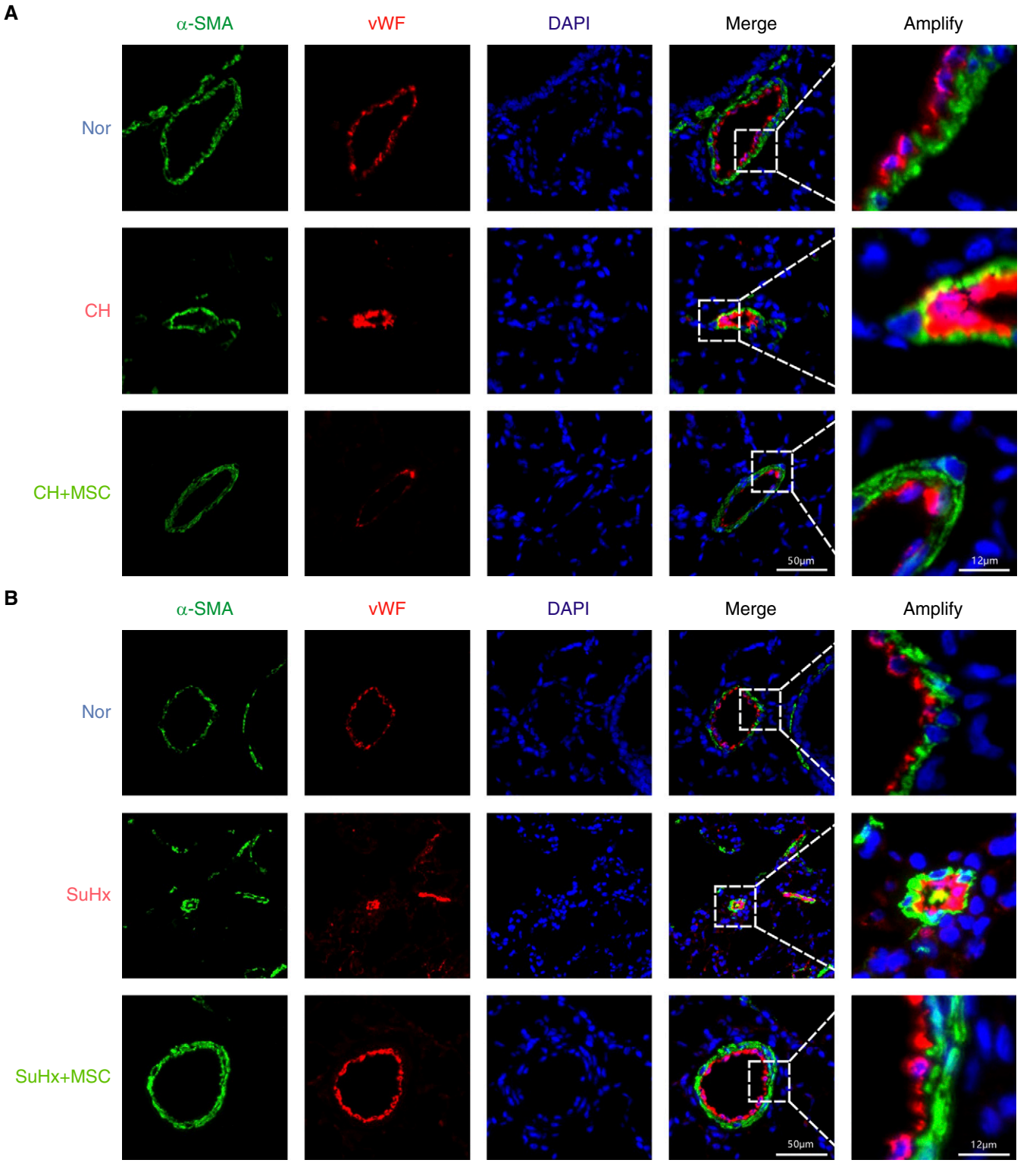

Figure 4. Endothelial-to-mesenchymal transition (EndMT) is present in the CHPH and SuHx-PH rat models. (*A* and *B*) Confocal laser microscopy analysis shows representative images of vWF (red) and α-SMA (green) double staining in lung sections from normal rats and CHPH/SuHx-PH models with or without MSC treatment. Double-positive staining for vWF and α-SMA are represented by yellow fluorescence ($n = 5$ in each group). Scale bars: 12 μm and 50 μm. α-SMA = α-smooth muscle actin.

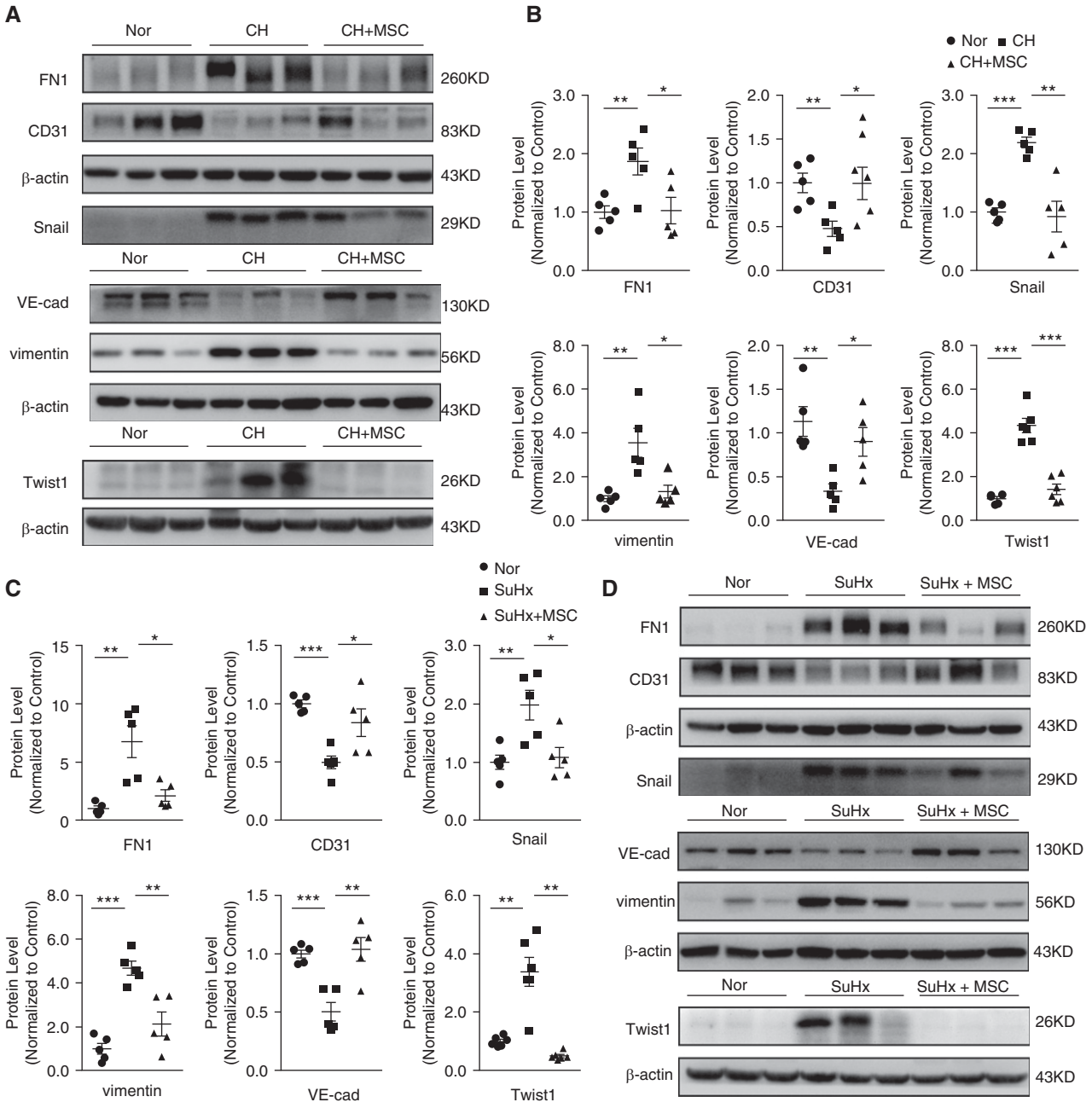

Figure 5. MSC reduced EndMT in the lung vasculature from both CHPH and SuHx-PH rats. (*A* and *D*) Western blot analysis shows FN (fibronectin) 1, CD31, Snail, Twist1, VE (vascular endothelial)-cadherin, and vimentin protein expression levels in lung tissues from CHPH (*A*) and SuHx-PH (*D*) models with or without MSC treatment. (*B* and *C*) Graphs show the quantification of FN1, CD31, Snail, Twist1, VE-cad, and vimentin protein expression levels normalized by β-actin protein expression measured from CHPH (*B*) and SuHx-PH (*C*) models with or without MSC treatment. Error bars represent means ± SEM ($n = 5$–6 in each group). $^{*}P < 0.05$, $^{**}P < 0.01$, and $^{***}P < 0.001$. VE-cad = VE-cadherin.

shown in Figures 7B and 7C, in primary cultured rat PMECs, we further demonstrated that MSCs could effectively reduce the protein half-life of HIF-2α, reflected by a cycloheximide chase experiment. Basically, we cocultured PMECs with MSC-CM in both the normoxia and hypoxia conditions, then the cells where maintained in the presence of cycloheximide (CHX; 20 μg/ml), which blocked protein synthesis. We found that HIF-2α was barely expressed under normoxic conditions with or without MSC-CM treatment (Figure 7B). While under hypoxic conditions, the expression of HIF-2α was upregulated, started to decrease within 20 minutes, and virtually disappeared within 1 hour after chase of CHX in the MSC-CM–treated group, which was obviously faster than the group without MSC-CM treatment (Figures 7B and 7C).

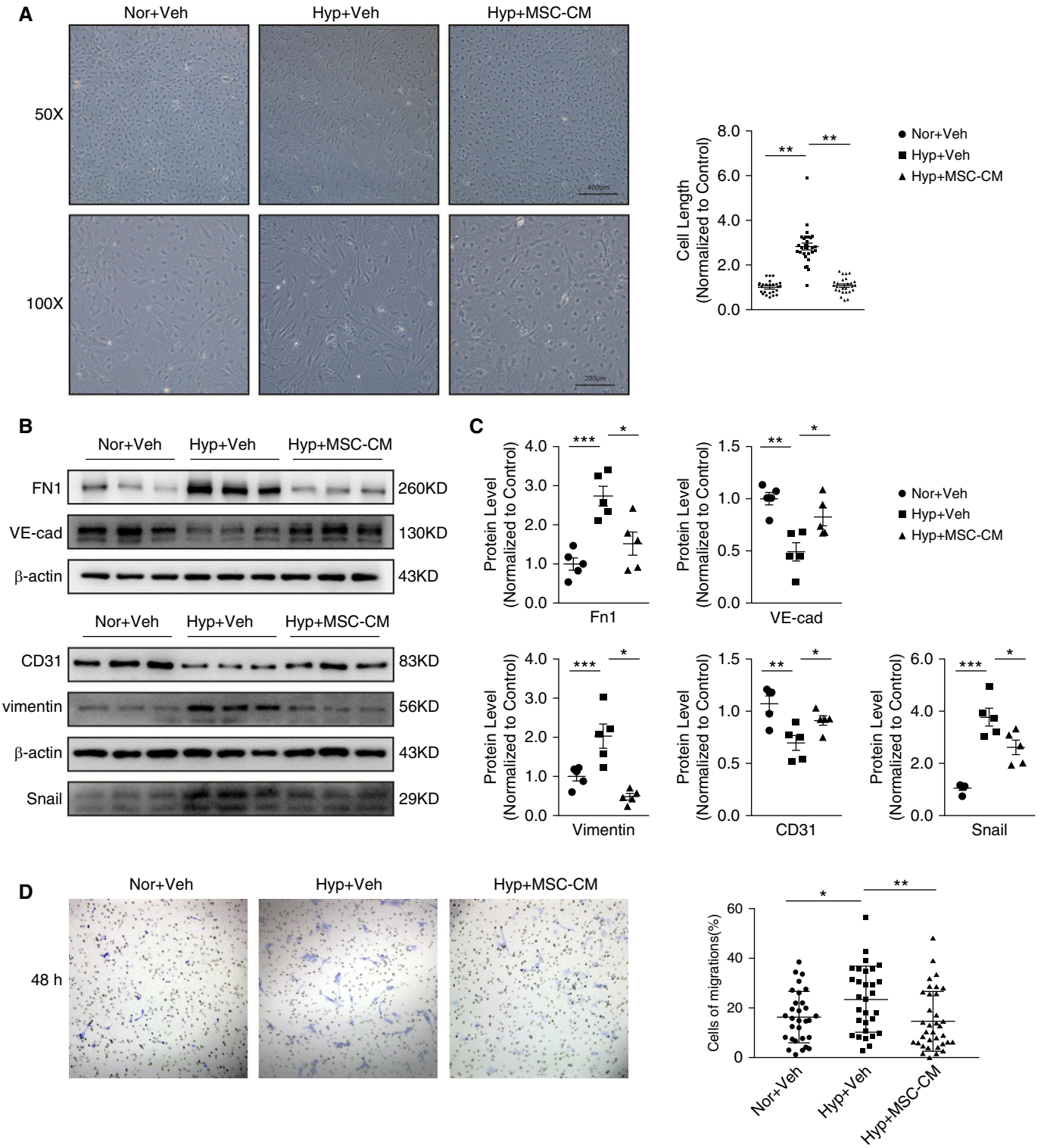

Figure 6. MSC conditioned medium (MSC-CM) attenuated hypoxia-induced EndMT in primary cultured pulmonary microvascular endothelial cells (PMECs). (*A*) Light microscopy analysis showing the morphologic changes (left panel) and summarized cell length (right panel) of PMECs treated with hypoxia control (Hyp + Veh) or with hypoxia and MSC-CM (Hyp + MSC-CM) simultaneously, compared with normoxia control cells (Nor + Veh). Western blots (*B*) and graphs (*C*) showing the protein expression levels of FN1, CD31, Snail, VE-cad, and vimentin in PMECs of normoxia control and hypoxia control with or without MSC treatment. (*D*) Cell migration was observed at 48 hours after transwell assay by light microscopy and calculated as the % migrated cells to total cells. Error bars represent means ± SEM ($n = 5$ in each group). $^{*}P < 0.05$, $^{**}P < 0.01$, and $^{***}P < 0.001$. Scale bars: 200 and 400 μm. Veh = vehicle.

Discussion

Recently, cell-based therapy has proven to be a promising approach for many human diseases, including PH, and has the potential to be a novel strategy for PH therapy. Promising preclinical investigations that examined the therapeutic potential of MSCs have demonstrated safety and efficacy, and provided the foundation for clinical trials. However, the underlying mechanisms are still poorly understood (7, 22). In the present study, we found that MSCs could reverse the PH pathogenesis in both the CHPH and SuHx-PH rat models, which was indicated by decreased mean RVSP, RV hypertrophy, and tunica media thickening of pulmonary arterioles. Interestingly, we have found that the treatment effects of MSCs on the SuHx-PH model is more significant than that in the CHPH model, which may indicate that the effects of MSCs might be related to the endothelial pathway. Therefore, we sought to determine whether MSC therapy could affect EndMT in the lung vasculature of experimental PH models, which showed protective effects.

Despite the *in vitro* and *in vivo* evidence for therapeutic effects of MSCs, the mechanisms by which MSCs exert their immunomodulatory and reparative effects remain unclear; however, this process likely involves multiple pathways, including direct effects (transdifferentiation and regeneration), paracrine effects, and immune regulatory effects (23). One of the characteristics of MSCs is their homing property to the sites of damaged tissue. Previous study has demonstrated that transplantation of MSCs could accumulate in the lung tissue and transform into vascular endothelial cells and SM cells, which may increase the total area of pulmonary vascular bed, improving the pulmonary blood supply, and effectively attenuating PH (9). However, other researchers reported that MSCs were not detected in the wall of pulmonary vessels,

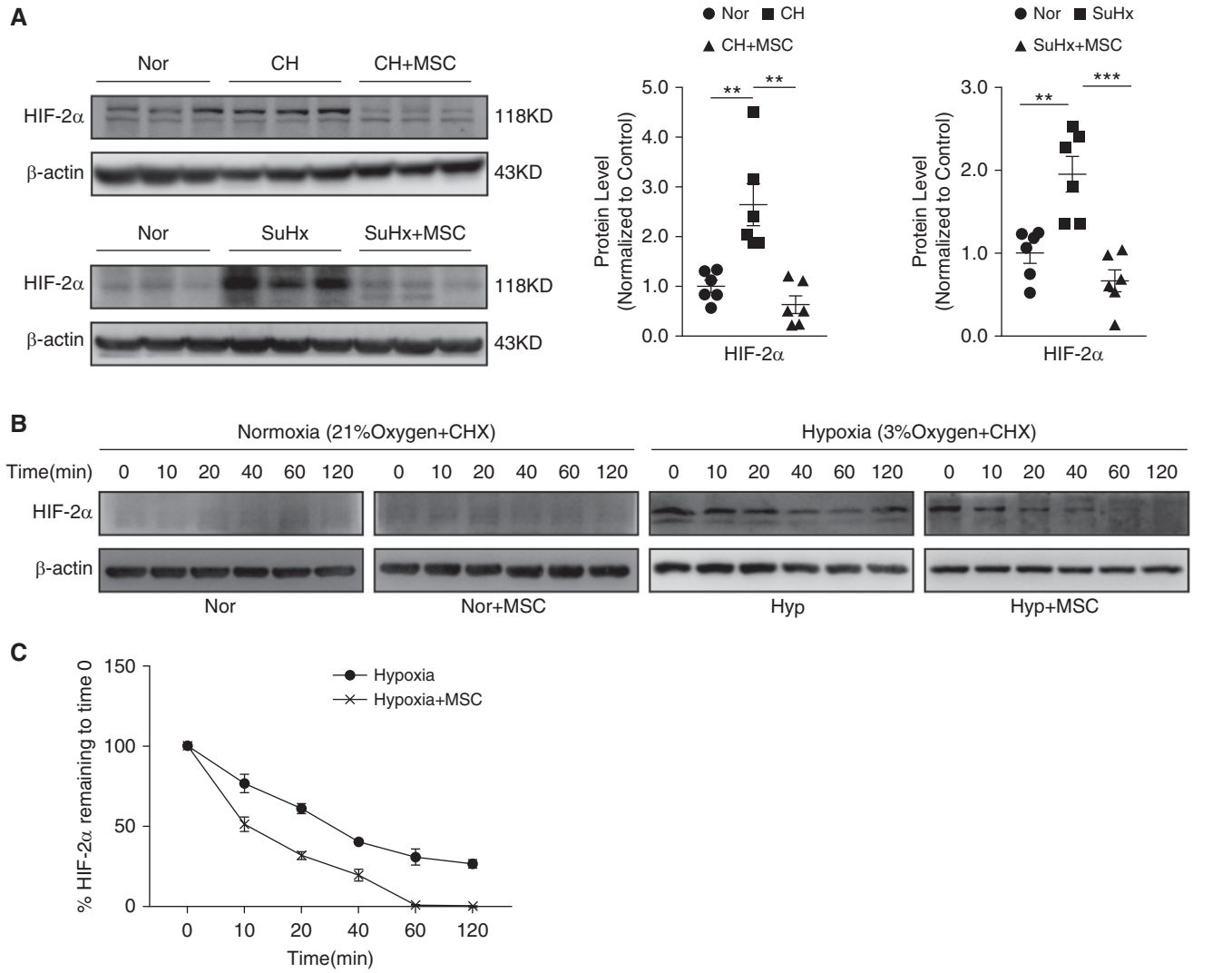

Figure 7. MSC-CM inhibited hypoxia-induced HIF-2α (hypoxia-inducible factor-2α) protein expression. (*A*) The protein expression of HIF-2α in lung tissues from CHPH (upper) and SuHx-PH (below) model with or without MSC treatment. Error bars represent means ± SEM ($n = 6$ in each group). $^{**}P < 0.01$ and $^{***}P < 0.001$. (*B*) PMECs were exposed for 72 hours to normoxia/hypoxia with/without MSC-CM. Then cells were maintained in the presence of cycloheximide. The protein expression levels of HIF-2α in PMECs were measured by Western blot. (*C*) The trace of HIF-2α protein degradation (% HIF-2α protein remaining to time 0). Points, mean from three experiments. Error bars represent means ± SEM ($n = 3$ in each group).

suggesting a potential role for a paracrine mechanism rather than for differentiation into vascular cells in the arterial wall (10). In this study, we continuously monitored GFP-labeled MSCs in the lung tissue at 3 hours, 1 day, 3 days, 7 days, and 14 days after intravenous injection, and found that MSCs homing to injured lung tissue reached peak at 7 days after transplantation, and gradually decreased in 2 weeks. By double staining, the transplanted cells were found located among the lung tissue rather than accumulated around the pulmonary vasculature, which suggests that MSCs might exert therapeutic effects through a paracrine mechanism rather than direct physical cell–cell contact and cell differentiation.

To date, the majority of cell therapy in PH studies was conducted in the MCT-PH rat model (8, 24). However, the MCT-PH model is not able to mimic the all the complex features observed in human PH. In contrast to the MCT-PH model, the SuHx-PH model establishes angio-obliterative lesions in the pulmonary arterioles, which yields more severe PH characteristics with more similar hemodynamic and histological features to human PH, especially in the plexiform lesions that are also found in human patients with idiopathic PA hypertension (25–27). By using the SuHx-PH rat model, our study, for the first time, evaluated the therapeutic potential of MSC transplantation. Because sugen is the inhibitor of VEGFR2, which is recently reported to be closely related to the EndMT process (26), our data, in combination, indicate that the protective roles of MSCs on PH might be due to its action on endothelial protection through normalizing EndMT. Notably, because MSC transplantation exerts significant preventive roles in attenuating the disease pathogenesis of both the CHPH and SuHx-PH models, we have also performed an interventional model study, in which MSCs were transplanted at Week 3 and lasted for 2 weeks (as seen in Figure E2A). However, compared with the prevention model (MSC transplantation at Week 1 and lasting for 2 wk), our results represent mild effects of MSCs on the disease pathogenesis of SuHx-PH models, suggesting that the effects of MSC transplantation on the reversal of established PH are less competitive, or requires a longer treatment course (Figure E3).

To date, although the pathogenesis of PH is not fully understood, endothelial dysfunction is widely recognized as the initial event of PH development, and then further manifested as some histological and functional abnormalities, such as intimal hyperplasia and fibrosis, medial SM cell hypertrophy and hyperplasia, extracellular matrix inflammatory cell infiltration, and/or increased collagen deposition caused by endothelial damage and dysfunction at the level of the intra-alveolar (precapillary) arteriole (26–28). In this study, we observed reduced EndMT in the lung vasculature of experimental PH models by immunofluorescence double-staining assay. We also observed significant upregulation of FN1, vimentin, Snail, and Twist1, and downregulation of VE-cadherin and PECAM-1 at the protein expression levels of lung tissue isolated from CHPH and SuHx-PH model rats, which can be largely normalized by the MSC treatment. The basal lamina is mainly composed of type IV collagen and laminin. The increased levels of MMPs lead to the excessive secretion of extracellular matrix composed of type I and type III collagen and FN, which promotes the cell motility (29). We also detected the collagen deposition in CHPH and SuHx rats, and found that these rats all represented obviously higher collagen deposition than control rats, which could be attenuated by the treatment of MSCs. Moreover, MSCs downregulated the increased expression of MMP2 and MMP9 in the lung tissue of model rats, as well as Collagen I and III. These observations strongly indicate that MSC treatment ameliorates the EndMT process *in vivo*.

In addition to the enhanced EndMT in rats with SuHx-induced PH, we also demonstrated that EndMT was enhanced in primary cultured PMECs when exposed to prolonged hypoxia. After an exposure to hypoxia for 7 days, the morphology of PMECs transformed from a cobblestone to a spindle-shaped, fibroblast-like appearance, and such phenotypic changes could be reversed by MSC-CM treatment. It has been hypothesized that EC apoptosis is also a trigger for the emergence of apoptosis-resistant and growth-dysregulated vascular cells (28, 29). Researchers have also reported that EndMT is present in the lung vascular endothelial cells from patients with idiopathic PA hypertension, which might account for the highly proliferative phenotype of these cells (18). Our data show that MSC-CM treatment could effectively reduce the migration and proliferation of PMECs, providing solid evidence that MSC treatment can suppress the EndMT process *in vitro*.

HIF-2α, a member of the HIF family, had been proven to be connected with EndMT in the previous study (5). In our experiments, we also found that MSC treatment could obviously attenuate the upregulation of HIF-2α at the protein levels of lung tissue isolated from both CHPH and SuHx-PH model rats. Therefore, we hypothesized that MSC treatment suppressed the EndMT process, likely, at least partly, by modulating the expression or activity of HIF-2α. Then, in cultured rat PMECs, we further demonstrated that treatment with MSC-CM significantly shortened the protein half-life of HIF-2α upon cotreatment with the protein synthesis inhibitor, CHX, indicating that MSCs could inhibit HIF-2α protein expression by promoting its protein degradation through the ubiquitin–proteasome system. However, the underlying mechanism remains unclear and needs further investigation.

In summary, in our study, we demonstrated that MSC transplantation represents the ideal therapeutic effects to inhibit PH pathogenesis in two well-established PH rat models (CHPH and SuHx-PH), likely by ameliorating the pulmonary vascular remodeling, inflammation, and EndMT. Moreover, in primary cultured PMECs, MSC-CM could also preserve the endothelial cell property by normalizing hypoxia-induced EndMT. Our data suggest that MSCs could be a potential therapeutic approach against PH, which deserves further evaluation and validation in our future studies. As far as we know, the present study is the first report to demonstrate that MSCs could inhibit EndMT in PH rats. However, the specific molecular mechanisms by which MSCs exert anti-EndMT function remain largely unknown, and require further determination. ■

Author disclosures are available with the text of this article at www.atsjournals.org.

References

1. Lai YC, Potoka KC, Champion HC, Mora AL, Gladwin MT. Pulmonary arterial hypertension: the clinical syndrome. *Circ Res* 2014;115:115–130.
2. Arciniegas E, Frid MG, Douglas IS, Stenmark KR. Perspectives on endothelial-to-mesenchymal transition: potential contribution to vascular remodeling in chronic pulmonary hypertension. *Am J Physiol Lung Cell Mol Physiol* 2007;293:L1–L8.
3. Stenmark KR, Frid M, Perros F. Endothelial-to-mesenchymal transition: an evolving paradigm and a promising therapeutic target in PAH. *Circulation* 2016;133:1734–1737.
4. Coll-Bonfill N, Musri MM, Ivo V, Barberà JA, Tura-Ceide O. Transdifferentiation of endothelial cells to smooth muscle cells play an important role in vascular remodelling. *Am J Stem Cells* 2015;4:13–21.
5. Tang H, Babicheva A, McDermott KM, Gu Y, Ayon RJ, Song S, *et al*. Endothelial HIF-2α contributes to severe pulmonary hypertension due to endothelial-to-mesenchymal transition. *Am J Physiol Lung Cell Mol Physiol* 2018;314:L256–L275.
6. Potenta S, Zeisberg E, Kalluri R. The role of endothelial-to-mesenchymal transition in cancer progression. *Br J Cancer* 2008;99:1375–1379.
7. Foster WS, Suen CM, Stewart DJ. Regenerative cell and tissue-based therapies for pulmonary arterial hypertension. *Can J Cardiol* 2014;30: 1350–1360.
8. de Mendonça L, Felix NS, Blanco NG, Da Silva JS, Ferreira TP, Abreu SC, *et al*. Mesenchymal stromal cell therapy reduces lung inflammation and vascular remodeling and improves hemodynamics in experimental pulmonary arterial hypertension. *Stem Cell Res Ther* 2017;8:220.
9. Luan Y, Zhang X, Qi TG, Cheng GH, Sun C, Kong F. Long-term research of stem cells in monocrotaline-induced pulmonary arterial hypertension. *Clin Exp Med* 2014;14:439–446.
10. Baber SR, Deng W, Master RG, Bunnell BA, Taylor BK, Murthy SN, *et al*. Intratracheal mesenchymal stem cell administration attenuates monocrotaline-induced pulmonary hypertension and endothelial dysfunction. *Am J Physiol Heart Circ Physiol* 2007;292:H1120–H1128.
11. Raoul W, Wagner-Ballon O, Saber G, Hulin A, Marcos E, Giraudier S, *et al*. Effects of bone marrow–derived cells on monocrotaline- and hypoxia-induced pulmonary hypertension in mice. *Respir Res* 2007;8:8.
12. Carrion FA, Figueroa FE. Mesenchymal stem cells for the treatment of systemic lupus erythematosus: is the cure for connective tissue diseases within connective tissue? *Stem Cell Res Ther* 2011;2:23.
13. Zhang Z, Wang JA, Xu Y, Jiang Z, Wu R, Wang L, *et al*. Menstrual blood derived mesenchymal cells ameliorate cardiac fibrosis via inhibition of endothelial to mesenchymal transition in myocardial infarction. *Int J Cardiol* 2013;168:1711–1714.
14. Choi HY, Lee HG, Kim BS, Ahn SH, Jung A, Lee M, *et al*. Mesenchymal stem cell–derived microparticles ameliorate peritubular capillary rarefaction via inhibition of endothelial–mesenchymal transition and decrease tubulointerstitial fibrosis in unilateral ureteral obstruction. *Stem Cell Res Ther* 2015;6:18.
15. Wang J, Weigand L, Lu W, Sylvester JT, Semenza GL, Shimoda LA. Hypoxia inducible factor 1 mediates hypoxia-induced TRPC expression and elevated intracellular Ca^{2+} in pulmonary arterial smooth muscle cells. *Circ Res* 2006;98:1528–1537.
16. Shimoda LA, Sham JS, Sylvester JT. Altered pulmonary vasoreactivity in the chronically hypoxic lung. *Physiol Res* 2000;49:549–560.
17. Lu W, Ran P, Zhang D, Peng G, Li B, Zhong N, *et al*. Sildenafil inhibits chronically hypoxic upregulation of canonical transient receptor potential expression in rat pulmonary arterial smooth muscle. *Am J Physiol Cell Physiol* 2010;298:C114–C123.
18. Ma R, Gong X, Jiang H, Lin C, Chen Y, Xu X, *et al*. Reduced nuclear translocation of serum response factor is associated with skeletal muscle atrophy in a cigarette smoke–induced mouse model of COPD. *Int J Chron Obstruct Pulmon Dis* 2017; 12:581–587.
19. Wang T, Satoh F, Morimoto R, Nakamura Y, Sasano H, Auchus RJ, *et al*. Gene expression profiles in aldosterone-producing adenomas and adjacent adrenal glands. *Eur J Endocrinol* 2011;164:613–619.
20. Lin MJ, Leung GP, Zhang WM, Yang XR, Yip KP, Tse CM, *et al*. Chronic hypoxia-induced upregulation of store-operated and receptor-operated Ca^{2+} channels in pulmonary arterial smooth muscle cells: a novel mechanism of hypoxic pulmonary hypertension. *Circ Res* 2004;95:496–505.
21. Suzuki T, Carrier EJ, Talati MH, Rathinasabapathy A, Chen X, Nishimura R, *et al*. Isolation and characterization of endothelial-to-mesenchymal transition cells in pulmonary arterial hypertension. *Am J Physiol Lung Cell Mol Physiol* 2018;314:L118–L126.
22. Martire A, Bedada FB, Uchida S, Pöling J, Krüger M, Warnecke H, *et al*. Mesenchymal stem cells attenuate inflammatory processes in the heart and lung via inhibition of TNF signaling. *Basic Res Cardiol* 2016;111:54.
23. Figueroa FE, Carrión F, Villanueva S, Khoury M. Mesenchymal stem cell treatment for autoimmune diseases: a critical review. *Biol Res* 2012; 45:269–277.
24. Luo L, Zheng W, Lian G, Chen H, Li L, Xu C, *et al*. Combination treatment of adipose-derived stem cells and adiponectin attenuates pulmonary arterial hypertension in rats by inhibiting pulmonary arterial smooth muscle cell proliferation and regulating the AMPK/BMP/Smad pathway. *Int J Mol Med* 2018;41:51–60.
25. Vitali SH, Hansmann G, Rose C, Fernandez-Gonzalez A, Scheid A, Mitsialis SA, *et al*. The Sugen 5416/hypoxia mouse model of pulmonary hypertension revisited: long-term follow-up. *Pulm Circ* 2014;4:619–629.
26. Sakao S, Taraseviciene-Stewart L, Cool CD, Tada Y, Kasahara Y, Kurosu K, *et al*. VEGF-R blockade causes endothelial cell apoptosis, expansion of surviving $CD34^+$ precursor cells and transdifferentiation to smooth muscle–like and neuronal-like cells. *FASEB J* 2007;21: 3640–3652.
27. Archer SL, Weir EK, Wilkins MR. Basic science of pulmonary arterial hypertension for clinicians: new concepts and experimental therapies. *Circulation* 2010;121:2045–2066.
28. Sakao S, Tatsumi K, Voelkel NF. Endothelial cells and pulmonary arterial hypertension: apoptosis, proliferation, interaction and transdifferentiation. *Respir Res* 2009;10:95.
29. Jurasz P, Courtman D, Babaie S, Stewart DJ. Role of apoptosis in pulmonary hypertension: from experimental models to clinical trials. *Pharmacol Ther* 2010;126:1–8.